# Stabilities of Negative Correlations between Blood Oxygen Level-Dependent Signals Associated with Sensory and Motor Cortices

**Lixia Tian,[1] Tianzi Jiang,[1]* Meng Liang,[1] Xiaobo Li,[1] Yong He,[2] Kun Wang,[1] Bingli Cao,[1] and Tao Jiang[3]***

[1]*National Laboratory of Pattern Recognition, Institute of Automation, Chinese Academy of Sciences, Beijing, P. R. China*
[2]*McConnell Brain Imaging Center, Montreal Neurological Institute, McGill University, Montreal, Quebec, Canada*
[3]*Department of Neurosurgery, Beijing Tiantan Hospital, Capital University of Medical Sciences, Beijing, P. R. China*

**Abstract:** Compared with positive correlations, negative correlations of blood oxygen level-dependent (BOLD) signals (NCOBSs) have been much less studied. In most related studies, the NCOBSs have been accepted as stable without further consideration. To investigate the stabilities of NCOBSs associated with the auditory, motor, and visual cortices, we evaluated the negative correlation maps of each brain region under different "task-backgrounds" within the same subject-group, as well as within different subject-groups during a conscious resting state. These "task-backgrounds" refer to tasks not expected to activate the specific ROI under consideration and are in some sense analogous to "resting states." We found that the negative correlation maps of the motor and visual cortices were quite variable between either different task-backgrounds or different subject-groups, whereas those of the auditory cortex exhibited some similarities. These results indicate that the NCOBSs associated with the motor and visual cortices were unstable both under task-backgrounds and during the conscious resting state. The auditory cortex tended to have stable NCOBSs during these "resting states" (but scanner noise could make the auditory cortex "less resting"). This study highlights the importance of paying attention to the influence of the stabilities of NCOBSs in related studies and establishes the need for further studies on NCOBSs. *Hum Brain Mapp 28:681–690, 2007.* ©2007 Wiley-Liss, Inc.

**Key words:** functional connectivity; positive correlation; resting state; task-background

## INTRODUCTION

Blood oxygen level-dependent (BOLD) functional MRI (fMRI) has been found to be a valuable tool in the investigation of functions such as perception and cognition in the human brain. Mechanisms of human brain function can be explored from two perspectives. One is by activation detection from the functional segregation perspective, that is, by detecting the brain activity patterns under given stimuli. The other is by functional connectivity analysis from the functional integration perspective, that is, by analyzing the temporal correlations between spatially separate brain regions [Friston et al., 1993].

Contract grant sponsor: Natural Science Foundation of China; Contract grant numbers: 30425004, 30570509, and 60121302; Contract grant sponsor: National Key Basic Research and Development Program (973); Contract grant number: 2003CB716100.

*Correspondence to: Tianzi Jiang, National Laboratory of Pattern Recognition, Institute of Automation, Chinese Academy of Sciences, Beijing 100080, P. R. China. E-mail: jiangtz@nlpr.ia.ac.cn or Tao Jiang, Department of Neurosurgery, Beijing Tiantan Hospital, Capital University of Medical Sciences, 6 Tiantan Xili, Beijing 100050, P. R. China. E-mail: jiangtao369@sohu.com

Received for publication 16 December 2005; Accepted 30 April 2006
DOI: 10.1002/hbm.20300
Published online 31 January 2007 in Wiley InterScience (www.interscience.wiley.com).

Positive correlations of BOLD signals (PCOBSs) have been widely used to measure the functional connectivities between brain regions for a large variety of research purposes [Arfanakis et al., 2000; Biswal et al., 1995; Cohen et al., 2005; Homae et al., 2003; Koshino et al., 2005; Peltier et al., 2005]. Compared with PCOBSs, negative correlations of BOLD signals (NCOBSs) seemed to have been much less noticed until pioneering studies were carried out by Fransson [2005] and Fox et al. [2005]. Both of those studies focused on brain regions that routinely exhibited task-related decreases in activity (e.g., posterior cingulate cortex (PCC)), and analyzed their resting state PCOBSs and NCOBSs. Interestingly, Fox et al. [2005] found not only coherent PCOBSs between brain regions within a "task-positive" network, as well as within a "task-negative" network, but also coherent NCOBSs between these two networks. Thus, Fox et al. suggested that NCOBSs might be as important as PCOBSs from the perspective of brain organization.

Although the NCOBSs between the "task-positive" and "task-negative" networks were observed to be consistent, and were regarded as intrinsic [Fox et al., 2005], the stabilities of NCOBSs associated with other networks or subsystems in the human brain have not been reported so far. In this study, we investigated the stabilities of NCOBSs associated with the regions of interest (ROIs) located at the auditory, motor, and visual cortices. We selected these three brain regions as ROIs for two reasons. One is that their functions are well known, and thus would facilitate our making deductions according to these known functions. The other is the "purity" of their functions, that is, each brain region fulfils uncomplicated functions, which would reduce the possible uncertainty or confusion that would be caused by selecting ROIs with multiple functions (e.g., prefrontal cortex). Stabilities of PCOBSs were also evaluated here simply for providing references for analyses of the stabilities of NCOBSs. We investigated the stabilities of NCOBSs associated with these ROIs from the following two aspects: First, in a group of normal subjects we examined the correlation maps of each ROI under different tasks that would not be expected to activate the specific ROI. These different tasks can be regarded as different backgrounds for the specific ROI, and thus will be referred to as "task-backgrounds." In the present study correlation maps of the auditory cortex were obtained based on the datasets acquired during a motor task as well as those acquired during a visual task; similarly, correlation maps of the motor cortex were obtained based on auditory-task datasets and the visual-task datasets; and the correlation maps of the visual cortex were obtained based on the auditory-task datasets and the motor-task datasets. We did this to investigate whether NCOBSs would be sensitive to task-backgrounds. Here these "task-backgrounds" are in some sense analogous to "resting states." Actually, as compared to conscious resting state, "task-backgrounds" can be regarded as "purer" "resting states," since the brain would be engaged in performing tasks, and thus these "resting states" would be more controlled. Second, to investigate whether NCOBSs would be sensitive to subject-groups, we examined the correlation maps of each ROI within two subject-groups from the same pool during a conscious resting state. We carried out correlational analysis during the "resting state" (as has been mentioned, task-backgrounds are in some sense analogous to the resting state), instead of during task performance, in order to reduce the dependence of the results on tasks and the variabilities accompanying the tasks, such as subjects' performance and the degree of involvement of brain regions into the given task [Arfanakis et al., 2000]. By doing this we expect to increase the universality of the present results.

## MATERIALS AND METHODS

Our correlational analyses were based on datasets acquired during auditory, motor, and visual processing (referred to as *Task data*), as well as during a conscious resting state (referred to as *Resting data*).

### Subjects and Protocols

#### *Task data*

Nine right-handed normal subjects (25.3 ± 2.8 years, three females) participated in the study after giving written informed consent in accordance with Beijing MRI Centre's Review Board. These subjects were recruited by advertisements. Each subject participated in all three task sessions (auditory, motor, and visual) that were arranged pseudorandomly during the scanning process. Each session consisted of experimental and control epochs that alternated every 30 s for 7 cycles and began with a control epoch. Thus, each session lasted for 420 s (not including the preceding 4 s of scanning that was discarded automatically by the scanner for the consideration of scanner instability). The subjects were instructed to open their eyes only during the visual processing task. The control portions were rest for the auditory and hand motion tasks, and looking at a cross for the visual task. During the experimental epochs of the auditory sessions the subjects were instructed to listen passively to pseudorandomly arranged single tones of 200, 400, 600, 800, 1,000, and 1,200 Hz lasting for 500 ms alternating with 500 ms of silence given by air-driven headphones. During the experimental epochs of the hand motion sessions the subjects made fists when they were given a sensory stimulus by the experimenters. This stimulus was made by touching the subject's right ankle with a pencil at a rate of about 1 Hz. The experimenters were instructed to give the stimulus from behind a screen so that they could not be seen by the subject. During the experimental epochs of the visual sessions the subjects were asked to view an 8-Hz reversing black-white checkerboard projected on a screen that could be seen by

the subjects through a mirror mounted on the MRI head-coil.

### *Resting data*

Seventeen right-handed normal subjects (24.1 ± 3.7 years, nine females) participated in the study after giving written informed consent in accordance with the Review Board of Second Xiangya Hospital. These subjects were recruited by advertisements. During the resting state the subjects were instructed to keep still with their eyes closed and not to think of anything in particular.

## Imaging Methods

### *Task data*

The task data were obtained using a Siemens (Erlangen, Germany) TRIO 3 T scanner at the Beijing MRI Center for Brain Research. A total of 210 volumes (not including the two volumes discarded by the scanner) of echo-planar images (EPI) sensitive to BOLD contrast were obtained axially for each session. The acquisition parameters were: 2000/30 ms (TR/TE), 32 slices, 3.0/0.75 mm (thickness/gap), 220 × 220 mm (FOV), 64 × 64 (resolution), 90° (flip angle). Other images not used in the present study will not be described here.

### *Resting data*

The resting data were obtained using a 1.5 T GE (Milwaukee, WI) scanner at the Institute of Mental Health, Second Xiangya Hospital. A total of 180 volumes of EPI images were obtained axially (2000/40 ms (TR/TE), 20 slices, 5/1 mm (thickness/gap), 240 × 240 mm (FOV), 64 × 64 (resolution), 90° (flip angle)). Other images not used in the present study will not be described here.

## Preprocessing

### *Task data*

The functional scans were first corrected for within-scan acquisition time differences between slices and realigned to the first volume to correct for interscan head motions. The realigned images were then spatially normalized to the stereotaxic coordinates of Talairach and Tournoux [1988] and resampled to 3 × 3 × 3 mm. Subsequently, the functional scans were spatially smoothed with an 8 × 8 × 8 mm full-width at half-maximum (FWHM) Gaussian kernel to decrease spatial noise. All these processes were conducted with SPM2 (http://www.fil.ion.ucl.ac.uk/spm/). Four possible sources of artifacts were removed from the data through linear regression [Fox et al., 2005; Salvador et al., 2005]. These were: 1) six head motion parameters; 2) the mean time series of all the voxels within a mask excluding voxels outside the brain; 3) linear trends; and 4) the possible influence of the tasks modeled by their hemodynamic response and their temporal derivatives. The waveform of each voxel was then passed through a band-pass filter (0.01–0.08 Hz) to reduce low-frequency drift and high-frequency noise using AFNI (http://afni.nimh.nih.gov/). Considering the susceptibility of correlational analysis to head motions, datasets with a mean head motion of greater than 0.4 mm (evaluated by the method in Jiang et al. [1995]) were discarded. Based on this criterion, datasets of one auditory session and one motor session were not usable.

### *Resting data*

The first 10 volumes of resting data were discarded to allow for scanner stabilization. The remaining preprocessing steps for resting data were identical to those for task data except that no possible task influence was considered when removing the possible artifacts, i.e., three possible sources of artifacts were considered here. One resting dataset was discarded using the same criterion as was used for the task data.

## ROIs

### *Task data*

A random-effect analysis [Holmes et al., 1998] was first performed to determine task-induced brain activities ($P < 0.001$, corrected). For the auditory task, left AI (Talairach coordinates [–56, –17, 6]) had the largest peak z-score; for the hand motion task, right MI ([42, –21, 54]) had the largest peak z-score; the visual task had the largest peak z-score at the right fusiform gyrus ([48, –50, –10]), which is not a region that is commonly recognized as specific for simple visual processing (our emphasis in this study), so we selected the left VII (Talairach coordinates [–27, –84, –2]) with the second largest peak z-score for further analysis. ROIs were defined as the 6-mm-radius spheres centered on the active foci.

### *Resting data*

For resting data, ROIs were defined as the 6-mm-radius spheres centered on the active foci found in task data. The mean time series of the ROIs were defined as the seed reference time course for further correlational analysis.

## Correlation Analysis

### *Task data*

For each ROI, correlational analyses were based on both of its task-background datasets. Pearson's correlation analyses were performed between the seed reference time courses and the time series from the whole brain in a voxelwise manner. This produced spatial maps in which the values of the voxels represented the strength of the correlation with the ROI. The correlation coefficients were finally transformed into z-scores using Fisher's transformation to improve normality [Press et al., 1992].

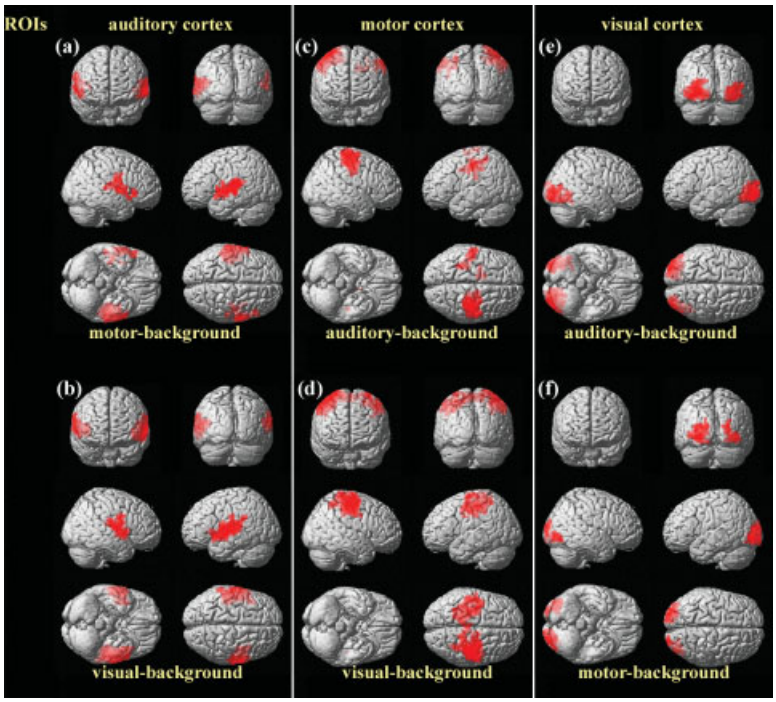


**Figure 1.**
Positive correlation maps of the auditory (**a,b**), motor (**c,d**), and visual (**e,f**) cortices under task-backgrounds (**c,e:** auditory-task-background; **a,f:** motor-task-background; **b,d:** visual-task-background). The statistical results were rendered onto a 3D brain reconstruction provided by SPM2. The threshold was set at $P < 0.001$ (corrected). Note the similarities in correlation patterns between (**a**) and (**b**), (**c**) and (**d**), as well as (**e**) and (**f**). [Color figure can be viewed in the online issue, which is available at www.interscience.wiley.com.]

### *Resting data*

Individual correlation maps for each ROI based on resting data were obtained in the same way as those based on task data.

## Statistical Analysis

### *Task data*

A random-effect [Holmes et al., 1998] one-tailed one-sample *t*-test was carried out to obtain within-group positive and negative correlation maps. The random-effect analysis estimates the error variance across subjects, rather than across scans. A combined threshold and clustering approach was performed to correct for multiple comparisons. Specifically, the combining of individual voxels' height threshold of $P < 0.001$ and a cluster size of at least 1,053 $mm^3$ (39 voxels $\times$ 27 $mm^3$) would yield a corrected *P*-value of $P < 0.001$, as indicated by performing 5,000 Monte Carlo simulations using AlphaSim (parameters: FWHM = 8 mm and a mask including 76,601 voxels) (Ward, http://afni.nimh.nih.gov/pub/dist/doc/manual/AlphaSim.pdf). The threshold for 11 of the 12 correlation maps (3 ROIs $\times$ 2 task-backgrounds $\times$ 2 correlation modes (positive and negative)) were set at 0.001 (corrected). The negative correlation map of the left VII under motor-background had no significant cluster at this threshold. For display convenience, we lowered the threshold for the map to a corrected $P < 0.01$ (individual voxel's $P < 0.005$, cluster size $>$ 1,566 $mm^3$ (58 voxels $\times$ 27 $mm^3$), determined by Monte Carlo simulations).

### *Resting data*

The 16 subjects were divided into two groups according to their acquisition order, with odd numbers in one group and even numbers in the other. These are referred to as *Group 1* and *Group 2*, respectively. A random-effect [Holmes et al., 1998] one-tailed one-sample *t*-test was carried out to obtain positive and negative correlation maps of each ROI for each subject-group. The threshold for all the 12 correlation maps (3 ROIs $\times$ 2 subject-groups $\times$ 2 correlation modes) was set at $P < 0.001$ (individual voxel's $P < 0.001$, cluster size $>$ 1,053 $mm^3$).

Since most of the brain regions exhibiting significant PCOBSs with our ROIs were cortical regions, the positive correlation maps were displayed by rendering statistical results onto a 3D brain reconstruction provided by SPM2. Brain regions exhibiting significant NCOBSs with our ROIs seemed to be more widespread and extended at times into subcortical regions, so the negative correlation maps were displayed within glass brains.

# RESULTS

## Correlation Maps Based on Task Data

The positive correlation maps of each ROI were quite consistent across different task-backgrounds (Fig. 1, Table I). Indeed, each ROI was strongly coupled with its contralateral counterpart under both task-backgrounds. The right MI was also positively correlated with the supplementary motor area (SMA) under the visual-background (Fig. 1d, Table I). No brain region in common was found in either

**TABLE I. Significant positive correlations with the auditory, motor, and visual cortices under task-backgrounds**

| ROI and region | Cluster size, $mm^3$ | BA | Talairach (peak) | T-score (peak) |
|---|---|---|---|---|
| Left AI | | | | |
| Motor task-background | | | | |
| L AI/AII/Insula | 16632 | 41/42/22/13 | −53, −14, 3 | 22.48 |
| R AII | 7911 | 22 | 59, 6, 5 | 11.96 |
| Visual task-background | | | | |
| L AI/AII/Insula | 24597 | 41/42/22/13 | −56, −20, 7 | 27.30 |
| R AI/AII/Insula | 12771 | 41/22/13 | 59, −11, 12 | 21.42 |
| Right MI | | | | |
| Auditory task-background | | | | |
| R MI/PreM | 20601 | 4/6 | 42, −23, 59 | 33.81 |
| L SI/MI | 5994 | 3/4 | −33, −38, 54 | 11.33 |
| B Cingulate[a] | 1350 | | −12, 5, 36 | 10.32 |
| Visual task-background | | | | |
| R MI/PreM/ | | 4/6 (R) | | |
| L SI/MI/ | 46521 | 3/4 (L) | 42, −21, 54 | 33.03 |
| B SMA | | 6 (B) | | |
| Left VII | | | | |
| Auditory task-background | | | | |
| L VII/VIII | 17307 | 18/19 | −30, −85, −1 | 27.26 |
| R VII/VIII | 10368 | 18/19 | 30, −73, −9 | 13.86 |
| Motor task-background | | | | |
| L VII | 8991 | 18 | −30, −85, −1 | 25.88 |
| R VI | 1350 | 17 | 24, −95, 19 | 15.71 |
| R VII | 3213 | 18 | 42, −73, −1 | 9.56 |

The threshold was set at $P < 0.001$ (corrected). ROI, region of interest; L, left; R, right; B, bilateral; BA, Brodmann's area; PreM, premotor; SMA, supplementary motor area.
[a] A large part of the cluster was white matter.

the two negative correlation maps of the motor cortex or the two maps of the visual cortex (Fig. 2c–f, Table II). The two negative correlation maps of the auditory cortex shared some resemblance (Fig. 2a,b, Table II). Specifically, the left superior frontal gyrus (SFG, BA8) and the medial frontal cortex (MedFC, BA8) appeared in both of these maps.

## Correlation Maps Based on Resting Data

Consistent positive correlation maps were also found across the two subject-groups (Fig. 3, Table III). Each ROI exhibited significant positive correlation with its contralateral counterpart in both groups. The right MI also exhibited significant positive correlations with the SMA in both

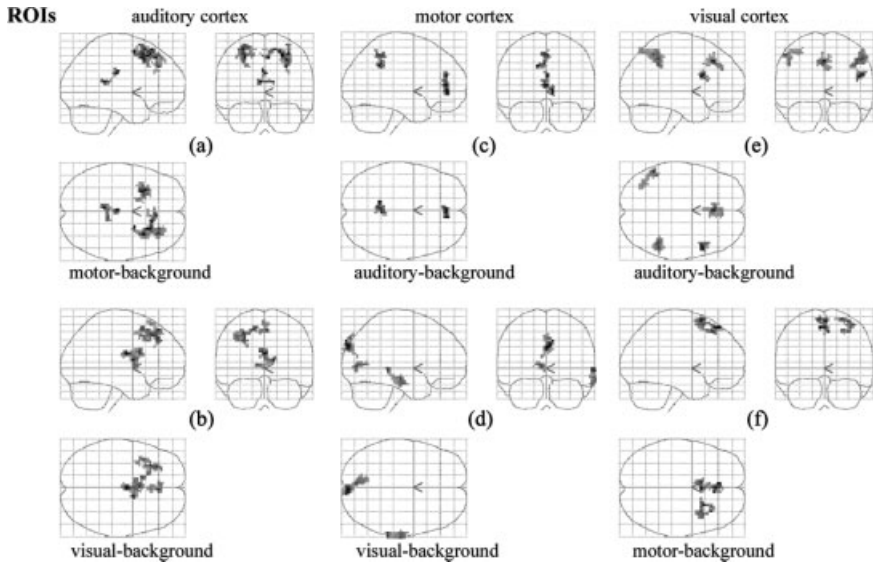


**Figure 2.**
Negative correlation maps of the auditory (**a,b**), motor (**c,d**), and visual (**e,f**) cortices under task-backgrounds **(c,e:** auditory-task-background; **a,f:** motor-task-background; **b,d:** visual-task-background). The statistical results were displayed within glass brains. The threshold was set at $P < 0.001$ (corrected) for (**a–e**), and $P < 0.01$ (corrected) for (**f**). Note the dissimilarities in anticorrelation patterns between (**c**) and (**d**), as well as (**e**) and (**f**).

**TABLE II. Significant negative correlations with the auditory, motor, and visual cortices under task-backgrounds**

| ROI and region | Cluster size, $mm^3$ | BA | Talairach (peak) | T-score (peak) |
|---|---|---|---|---|
| Left AI | | | | |
| Motor task-background | | | | |
| B CC[b] | 1242 | | −3, −19, 29 | 11.70 |
| R SFG/MedFC | 5643 | 6/8 | 30, 17, 41 | 11.32 |
| L SFG | 3591 | 8 | −30, 20, 54 | 10.77 |
| Visual task-background | | | | |
| B CC/Caudate[b] | 3483 | | 0, −8, 20 | 11.34 |
| B MedFC | 1107 | 8 | 3, 37, 48 | 8.42 |
| L MFG/SFG | 3024 | 8 | −30, 34, 45 | 8.00 |
| Right MI | | | | |
| Auditory task-background | | | | |
| B PCC/ Precuneus | 1674 | 31 | −12, −45, 35 | 8.26 |
| B ACC | 1701 | 24 | 0, 44, 6 | 7.81 |
| Visual task-background | | | | |
| B Cuneus | 2025 | 19 | 6, −86, 35 | 8.96 |
| R MTG | 1863 | 21 | 62, −35, 2 | 7.03 |
| B Cuneus/PCC | 1215 | 17/30 | −6, −75, 7 | 6.58 |
| Left VII | | | | |
| Auditory task-background | | | | |
| R IFG | 1188 | 9 | 50, 16, 21 | 11.33 |
| B MedFC | 2349 | 10 | 0, 31, 37 | 9.87 |
| L IPL | 2025 | 40 | −53, −50, 49 | 8.86 |
| R IPL | 2349 | 40 | 50, −42, 44 | 8.21 |
| Motor task-background[a] | | | | |
| B MedFC | 1998 | 8 | −6, 37, 51 | 7.19 |
| R SFG | 1836 | 6 | 24, 18, 63 | 6.06 |

The threshold was set at $P < 0.001$ (corrected). ROI, region of interest; L, left; R, right; B, bilateral; BA, Brodmann's area; CC, corpus callosum; SFG, superior frontal gyrus; IPL, inferior parietal lobe; MFG, middle frontal gyrus; IFG, inferior frontal gyrus; MTG, middle temporal gyrus; ACC, anterior cingulate cortex; PCC, posterior cingulate cortex; MedFC, medial frontal cortex.

[a] A large part of the cluster was white matter.

[b] The threshold was set at $P < 0.01$ (corrected).

groups (Fig. 3c,d, Table III). In addition, a small cluster in the bilateral cuneus was also found to exhibit significant positive correlation with the left AI in Group 2 (Fig. 3b, Table III). No brain region in common was found in the two negative correlation maps of the motor cortex (Fig. 4c,d, Table IV). Left VII was significantly anticorrelated with the left angular gyrus (AG, BA39) in both groups, but with the bilateral precuneus (BA7) and the bilateral MedFC (BA9) only in Group 1, and with the right AG/middle temporal gyrus (MTG, BA37) only in Group 2 (Fig. 4e,f, Table IV). Again, the two negative correlation maps of the auditory cortex shared some resemblance (Fig. 4a,b, Table IV): bilateral SFG (BA8) appeared in both of the maps.

## DISCUSSION

In this study we evaluated the NCOBSs associated with the auditory, motor, and visual cortices within the same subject-group under different task-backgrounds, as well as within different subject-groups during a conscious resting state, to investigate their stabilities. We found that the negative correlation maps of the motor and visual cortices were quite variable across either different task-backgrounds or different subject-groups (Figs. 2c–f, 4c–f, Tables II, IV), while those of the auditory cortex shared some similarities (Figs. 2a,b, 4a,b, Tables II, IV).

Correlational analysis is sensitive to such "systemic noises" as head motions and whole-brain signals, which may globally increase the correlation coefficients. In this study the influences of several possible sources of artifacts, such as head-motion effects, whole-brain signals, and task-induced signal changes, were carefully removed by linear regression. This processing may facilitate our finding relatively more reliable NCOBSs.

The four positive correlation maps of each ROI were quite consistent. The functions of the brain regions appearing in these maps were closely related to those of the given ROI. Moreover, few outliers were found in these maps. Specifically, significant PCOBSs with the left visual cortex were found only in the right visual cortex in all four positive correlation maps (Figs. 1e,f, 3e,f, Tables I, III). The right motor cortex had significant PCOBSs only with the left motor cortex (Figs. 1c,d, 3c,d, Tables I, III), sometimes extending to the SMA (Fig. 3b–d, Tables I, III). The left

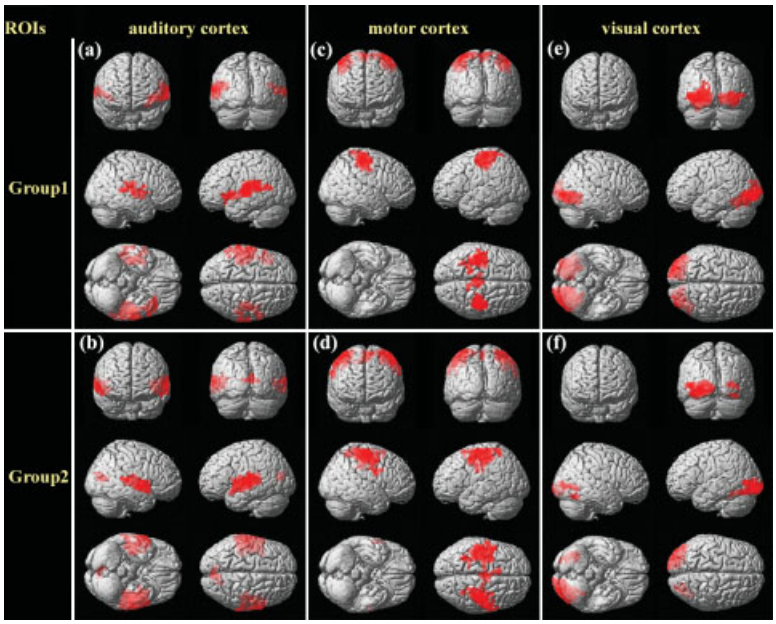


**Figure 3.**
Positive correlation maps of the auditory (**a,b**), motor (**c,d**), and visual (**e,f**) cortices during resting state. **a,c,e:** The maps for Group 1. **b,d,f:** The maps for Group 2. The statistical results were rendered onto a 3D brain reconstruction provided by SPM2. The threshold was set at $P < 0.001$ (corrected). Note the similarities in correlation patterns between (**a**) and (**b**), (**c**) and (**d**), as well as (**e**) and (**f**). [Color figure can be viewed in the online issue, which is available at www.interscience.wiley. com.]

auditory cortex showed significant PCOBSs only with the right auditory cortex in all four positive correlation maps (Figs. 1a,b, 3a,b, Tables I, III), except that a small cluster in bilateral cuneus appeared in Figure 3b. These findings were also consistent with those in former functional connectivity studies carried out either during the conscious resting state [Biswal et al., 1995; Cordes et al., 2001; Lowe et al., 1998], or under task-backgrounds [Arfanakis et al., 2000]. These consistencies provided evidence not only for the stabilities of PCOBSs associated with the present ROIs,

**TABLE III. Significant positive correlations with the auditory, motor, and visual cortices during resting state**

| ROI and region | Cluster size, $mm^3$ | BA | Talairach (peak) | T-score (peak) |
|---|---|---|---|---|
| Left AI | | | | |
| Group 1 | | | | |
| R AI/Insula | 8262 | 41/13 | 42, −19, 20 | 14.88 |
| L AI/AII | 22815 | 41/42/22 | −53, −17, 4 | 14.24 |
| Group 2 | | | | |
| L AI/AII/Insula | 22653 | 41/22/13 | −59, −20, 7 | 17.23 |
| R AI/AII | 12906 | 41/22 | 53, −6, −2 | 16.56 |
| B Cuneus | 2349 | 18 | 9, −69, 15 | 8.04 |
| Right MI | | | | |
| Group 1 | | | | |
| R SI/MI | 12069 | 3/4 | 42, −24, 51 | 19.64 |
| L SI/MI | 14013 | 3/4 | −39, −17, 62 | 14.73 |
| B SMA | 3186 | 6 | 9, −37, 71 | 9.87 |
| Group 2 | | | | |
| R SI/MI | 20952 | 3/4 | 45, −20, 56 | 25.73 |
| L SI/MI/SMA | 25731 | 3/4/6 | −50, 8, 47 | 12.74 |
| Left VII | | | | |
| Group 1 | | | | |
| L VII/VIII | 28512 | 18/19 | −30, −84, 7 | 37.06 |
| R VII/VIII | 18171 | 18/19 | 27, −76, 4 | 14.12 |
| Group 2 | | | | |
| L VII/VIII | 20088 | 18/19 | −45, −87, 2 | 27.01 |
| R Fusiform | 1323 | 19 | 36, −59, −12 | 16.53 |
| R VIII | 2403 | 19 | 30, −78, 4 | 9.24 |

The threshold was set at $P < 0.001$ (corrected). ROI, region of interest; L, left; R, right; B, bilateral; BA, Brodmann's area; SMA, supplementary motor area.

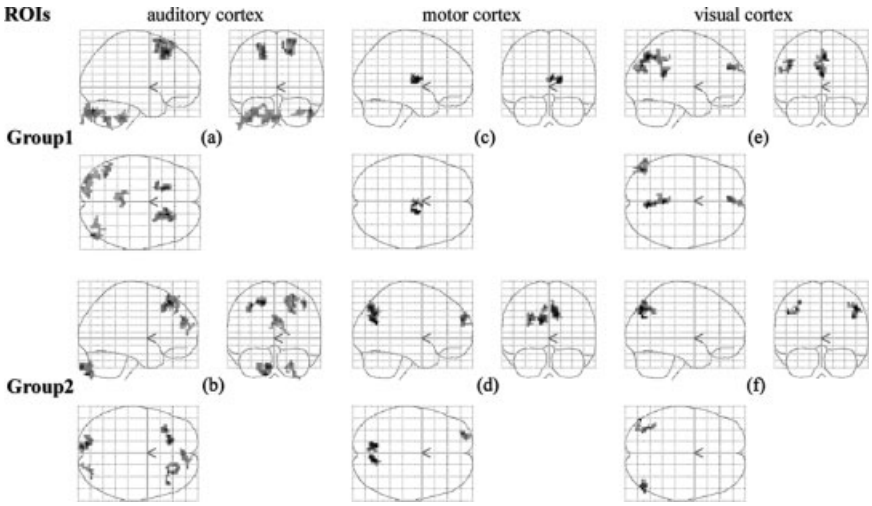


**Figure 4.**
Negative correlation maps of the auditory (**a,b**), motor (**c,d**), and visual (**e,f**) cortices during resting state. **a,c,e:** The maps for Group 1. **b,d,f:** The maps for Group 2. The statistical results were displayed within glass brains. The threshold was set at $P < 0.001$ (corrected). Note the dissimilarities in anticorrelation patterns between (**c**) and (**d**), as well as (**e**) and (**f**).

but also for the reliability of the present datasets and analysis methods, i.e., the resultant negative correlation maps acquired from these datasets and analysis methods are expected to be reliable.

The negative correlation maps associated with the motor and visual cortices obtained in the present study were quite variable (Figs. 2c–f, 4c–f, Tables II, IV). The four negative correlation maps associated with the right MI shared

**TABLE IV. Significant negative correlations with the auditory, motor, and visual cortices during resting state**

| ROI and region | Cluster size, $mm^3$ | BA | Talairach (peak) | T-score (peak) |
|---|---|---|---|---|
| Left AI | | | | |
| Group 1 | | | | |
| R SFG | 4185 | 8 | 18, 26, 46 | 14.31 |
| R Cerebellum | 2133 | | 48, −80, −24 | 11.34 |
| L SFG | 2484 | 8 | −18, 23, 46 | 10.93 |
| L Cerebellum | 1647 | | −39, −63, −35 | 8.77 |
| B Brainstem | 1944 | | −3, −40, −36 | 8.29 |
| L Cerebellum | 3591 | | −36, −86, −23 | 8.02 |
| Group 2 | | | | |
| L SFG | 2160 | 8 | −15, 34, 45 | 11.95 |
| L Cerebellum[a] | 2349 | | −12, −86, −39 | 10.15 |
| R SFG | 2700 | 8/9 | 42, 31, 45 | 9.11 |
| B MedFC | 1539 | 8/9 | 3, 51, 22 | 7.69 |
| R Cerebellum | 1188 | | 24, −83, −26 | 7.28 |
| Right MI | | | | |
| Group 1 | | | | |
| R Thalamus | 1539 | | 18, −5, 11 | 7.09 |
| Group 2 | | | | |
| L Precuneus | 1755 | 31 | −12, −66, 25 | 10.72 |
| R Precuneus | 1917 | 7 | 9, −65, 34 | 10.00 |
| L SFG | 1134 | 10 | −27, 56, 22 | 9.49 |
| Left VII | | | | |
| Group 1 | | | | |
| B Precuneus | 3510 | 7 | 6, −65, 42 | 9.64 |
| L AG/MTG | 1917 | 39 | −45, −71, 31 | 8.63 |
| B MedFC | 1080 | 9 | −6, 48, 22 | 8.25 |
| Group 2 | | | | |
| R AG/MTG | 1323 | 37 | 48, −73, 45 | 8.98 |
| L AG/Precuneus/SPL | 1296 | 7/19/39 | −48, −74, 37 | 8.66 |

The threshold was set at $P < 0.001$ (corrected). ROI, region of interest; L, left; R, right; B, bilateral; BA, Brodmann's area; SFG, superior frontal gyrus; AG, angular gyrus; MTG, middle temporal gyrus; MedFC, medial frontal cortex; SPL, superior parietal lobe.
[a] A large part of the cluster was out of the brain.

no resemblance (Figs. 2c,d, 4c,d). Among the four negative correlation maps associated with the left VII, the only brain region in common appeared in the left AG within two of the maps (Figs. 2e,f, 4e,f). These highly variable negative correlation maps can be appropriate evidence for the instabilities of NCOBSs associated with the motor and visual cortices.

The four negative correlation maps of the left AI shared some similarities, since the bilateral SFG appeared in three of the four maps and the left SFG in another (Figs. 2a,b, 4a,b). These similarities indicate that the auditory cortex tended to have stable NCOBSs during these "resting states" (task-backgrounds and conscious resting state). However, it should be noticed that the scanner noises may perhaps make the auditory cortex less "resting," so conclusions drawn from the present results related to the auditory cortex would be less suitable for "resting states."

In the study by Fox et al. [2005], the NCOBSs between the "task-positive" and "task-negative" networks were quite stable and were regarded as "intrinsic"; whereas in the present study the NCOBSs associated with the motor and visual cortices were unstable. Neither of these two studies can clearly elucidate the factors that decide the stabilities of NCOBSs throughout the whole brain. Although it remains unknown whether stable NCOBSs are only limited to the "task-positive" and "task-negative" networks [Fox et al., 2005], or whether unstable NCOBSs only belong to those associated with the motor and visual cortices, some speculation about the stabilities of NCOBSs exists. First, as noted by Fox et al. [2005], the brain regions included in the "task-positive" and "task-negative" networks are "higher-order brain structures," whereas brain regions such as the motor and visual cortices are not as high order in that they are not primarily involved in cognitive processing. Hence, the stabilities of NCOBSs may depend on the complexity of functions of specific brain regions. Second, several brain regions that appeared in the "task-negative" network in the study by Fox et al. [2005], such as PCC and MedFC, have been demonstrated to be more metabolically active than other brain regions during a conscious resting state [Raichle et al., 2001]. The motor and visual cortices are less likely to be activated under task-backgrounds as well as during a conscious resting state. Thus, it may be possible that the stabilities of NCOBSs depend on the activity level of specific brain regions. Third, a combination of the above two situations may decide the stabilities of NCOBSs, that is, only active "high-order" brain regions are likely to have stable NCOBSs.

As has been mentioned, the present results related to the auditory cortex would be not as representative for the "resting states" because the cortex is "less resting." However, two characteristics of the auditory cortex may be helpful in understanding the determinants of the stabilities of NCOBSs: the auditory cortex is of low-order brain function (as are the motor and visual cortices) and is relatively active during these "resting states" due to the scanner noises. So its tendency to have stable NCOBSs may imply that the stabilities of NCOBSs depend on the activity level of specific brain regions. Further studies are needed to test this hypothesis.

The problem of stabilities of NCOBSs is of great importance for functional connectivity analyses, especially for those based on a relatively small sample size, as was the case in the present study. At such small sample sizes the influences of the unstable NCOBSs would not be concealed by statistical "averaging," and thus these unstable NCOBSs could possibly lead to spurious conclusions. For instance, when comparing the correlation maps of the same ROI of two subject-groups, spurious between-group differences could be produced by occasional NCOBSs that occur in only one subject-group, as a result of the instabilities of NCOBSs. This highlights the importance of caution in interpreting results when NCOBSs occurred in cases in which their stabilities are not clear.

The present study was based on datasets obtained from two fMRI scanners of different field strengths, due to the limited availability of datasets. Acquiring a dataset with a larger sample size both under task-backgrounds and during a conscious resting state from the same scanner could permit us to investigate the consistencies of NCOBSs across different "resting states" and different subject-groups simultaneously. Moreover, a dataset obtained from the same scanner could avoid possible slight differences caused by field strength differences between the correlations maps. However, field strength differences would not be expected to have a serious impact on our findings, since similar stability characteristics of NCOBSs were also found between the negative correlation maps based on datasets from the same scanner. Accordingly, the present results based only on these available datasets seem sufficient to investigate the stabilities of NCOBSs associated with the brain regions we investigated.

Another potential source of artifact was that the cardiac and respiratory fluctuations could be aliased into the BOLD signals due to the low sampling rate (0.5 Hz) we adopted in the present study. These aliasing-effects could perhaps confound the resultant correlation patterns [Bhattacharyya et al., 2004; Dagli et al., 1999], that is, the aliasing-effects could be a source of the instabilities of NCOBSs. However, we suggest that the instabilities of NCOBSs observed in the present study were unlikely to be mainly caused by these aliasing-effects for the following two reasons. First, if the unstable NCOBSs observed in the present study were mainly caused by aliasing-effects, it would be difficult to understand why these aliasing-effects did not produce as many PCOBS differences as NCOBS differences, since aliasing-effects seem unlikely to influence these two correlation patterns differently. Second, we tried to reduce the influence of the "whole-brain signals" while performing data preprocessing, and we think that this process might also partially remove the aliasing-effects included in these whole-brain signals. This suggestion needs to be confirmed by studies in which the respiratory and cardiac cycles are simultaneously recorded.

Besides the problem of stability, there are still two things unclear about NCOBSs. First, little is known about the cause of NCOBSs, although PCOBSs have been suggested to be aroused by synchronous neuronal activities [Biswal et al., 1995]. The cause of NCOBSs may at least partially influence their stabilities. It should also be noticed that although task-backgrounds were treated as analogous to "resting states" in the present study, they may be fundamentally different from the conscious resting state in the usual sense of the term with regard to NCOBSs (because the cause of NCOBSs is unknown as yet), even though they are with PCOBSs. Second, the roles of NCOBSs in brain functions are far from clear. By analogy with the "functional integration" roles of PCOBSs, Fox et al. [2005] suggested that NCOBSs might subserve "functional differentiation" roles. Further studies are needed to investigate these two issues.

This study was the first to question the stabilities of NCOBSs. Our results indicate that the NCOBSs associated with the motor and visual cortices were unstable, whereas those associated with the auditory cortex tended to be stable. Although the stabilities of NCOBSs within the whole brain are still far from clear, we suggest that our work is significant in highlighting the importance of paying attention to the possible effects aroused by the instabilities of NCOBSs in related studies.

## ACKNOWLEDGMENTS

The authors thank the anonymous referees for significant and constructive comments and suggestions, which greatly improved the article. The authors also thank Drs. Rhoda E. and Edmund F. Perozzi of Beijing University of Technology for extensive English language assistance.

## REFERENCES

Arfanakis K, Cordes D, Haughton VM, Moritz CH, Quigley MA, Meyerand ME (2000): Combining independent component analysis and correlation analysis to probe interregional connectivity in fMRI task activation datasets. Magn Reson Imaging 18:921–930.

Bhattacharyya PK, Lowe MJ (2004): Cardiac-induced physiologic noise in tissue is a direct observation of cardiac-induced fluctuations. Magn Reson Imaging 22:9–13.

Biswal B, Yetkin FZ, Haughton VM, Hyde JS (1995): Functional connectivity in the motor cortex of resting human brain using echo-planar MRI. Magn Reson Med 34:537–541.

Cohen MX, Heller AS, Ranganath C (2005): Functional connectivity with anterior cingulate and orbitofrontal cortices during decision-making. Cogn Brain Res 23:61–70.

Cordes D, Haughton VM, Arfanakis K, Carew JD, Turski PA, Moritz CH, Quigley MA, Meyerand ME (2001): Frequencies contributing to functional connectivity in the cerebral cortex in "resting-state" data. Am J Neuroradiol 22:1326–1333.

Dagli MS, Ingeholm ,JE, Haxby JV (1999): Localization of cardiac-induced signal change in fMRI. Neuroimage 9:407–415.

Fox MD, Snyder AZ, Vincent JL, Corbetta M, Essen DCV, Raichle ME (2005): The human brain is intrinsically organized into dynamic, anticorrelated functional networks. Proc Natl Acad Sci U S A 102:9673–9678.

Fransson P (2005): Spontaneous low-frequency BOLD signal fluctuations—an fMRI investigation of the resting-state default mode of brain function hypothesis. Hum Brain Mapp 26:15–29.

Friston KJ, Frith CD, Liddle PF, Frackowiak RSJ (1993): Functional connectivity: the principal component analysis of large (PET) data sets. J Cereb Blood Flow Metab 13:5–14.

Holmes AP, Friston KJ (1998): Generalisability, random effects and population inference. Neuroimage 7:754.

Homae F, Yahata N, Sakai KL (2003): Selective enhancement of functional connectivity in the left prefrontal cortex during sentence processing. Neuroimage 20:578–586.

Jiang A, Kennedy DN, Baker JR, Weisskoff RM, Tootell RB, Woods RP, Benson RR, Kwong KK, Brady TJ, Rosen BR, Belliveau JW (1995): Motion detection and correction in functional MR imaging. Hum Brain Mapp 3:224–235.

Koshino H, Carpenter PA, Minshew NJ, Cherkassky VL, Keller TA, Just MA (2005): Functional connectivity in an fMRI working memory task in high-functioning autism. Neuroimage 24:810–821.

Lowe MJ, Mock BJ, Sorenson JA (1998): Functional connectivity in single and multislice echoplanar imaging using resting-state fluctuations. Neuroimage 7:119–132.

Peltier SJ, LaConte SM, Niyazov DM, Liu JZ, Sahgal V, Yue GH, Hu XP (2005): Reductions in interhemispheric motor cortex functional connectivity after muscle fatigue. Brain Res 1057:10–16.

Press WH, Teukolsky SA, Vetterling WT, Flannery BP (1992): Numerical recipes in C, 2nd ed. Cambridge, UK: Cambridge University Press.

Raichle ME, MacLeod AM, Snyder AZ, Powers WJ, Gusnard DA, Shulman GL (2001): A default mode of brain function. Proc Natl Acad Sci U S A 98:676–682.

Salvador R, Suckling J, Schwarzbauer C, Bullmore E (2005): Undirected graphs of frequency-dependent functional connectivity in whole brain networks. Philos Trans R Soc Lond B 360: 937–946.

Talairach J, Tournoux P (1988): Co-planar stereotaxic atlas of the human brain. New York: Thieme Medical.